
Radiative data calculations for electric dipole transitions in the Yb I isoelectronic sequence (Ta IV - Pt IX) of interest to nuclear fusion diagnostics

Maxime Brasseur

ComAS 2025, Lund, Sweden

June 12 2025

Table of contents

1. Introduction
 - Ionic impurities in the fusion plasma
 - Plasma diagnostics
2. HFR+CPOL preliminary results
 - Pseudo-relativistic Hartree-Fock method with the core polarization corrections (HFR+CPOL)
 - Model + least squares adjustment
 - Radiative decay rates
 - The configuration interactions and the core-valence correlations
3. MCDHF preliminary results
 - Multiconfigurational Dirac-Hartree-Fock (MCDHF) method
 - Model and convergence
 - Radiative decay rates (comparisons)

Introduction

Ionic impurities in the fusion plasma

- Divertor will be made of tungsten: high fluxes of heat and particles (neutrons)
- Transmutation products after few years irradiation time: rhenium, osmium, tantalum, hafnium, iridium and platinum → impurities
- Brittleness of pure tungsten → alloying elements (tantalum, rhenium, titanium or vanadium)

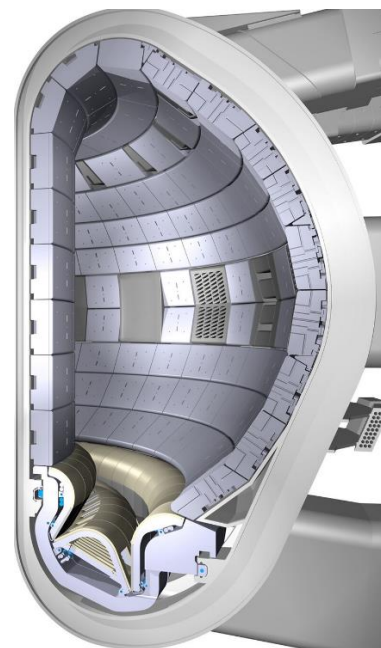
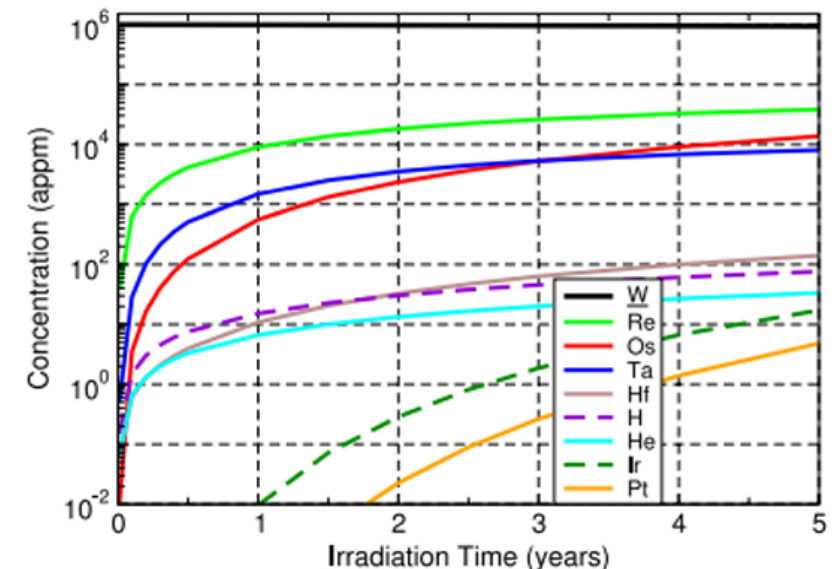


Illustration of the inside of the Tokamak.
(<https://encyclopedia.pub/entry/37629>)



Evolution of the concentration (Atomic Part Per Millions) of all the elements produced by the transmutation of W for a five-years irradiation [Gilbert, M. R and Sublet, J.Ch , 2011]

Plasma diagnostics

- Ionic impurities will contribute to the radiation losses/allow to diagnose the fusion plasma
- From observed intensity ratio and radiative parameters [H.J. Kunze, 2009] :

$$\Rightarrow \frac{\varepsilon_z(p \rightarrow q)}{\varepsilon_z(p' \rightarrow q')} = \frac{\lambda_{p'q'}}{\lambda_{pq}} \frac{A_z(p \rightarrow q)}{A_z(p' \rightarrow q')} \frac{A_z(p' \rightarrow)}{A_z(p \rightarrow)} \frac{X_z(g \rightarrow p)(T_e)}{X_z(g \rightarrow p')(T_e)} \Rightarrow T_e$$

$$\Rightarrow \frac{\varepsilon_z(p \rightarrow q)}{\varepsilon_z(p' \rightarrow q')} = \frac{\lambda_{p'q'}}{\lambda_{pq}} \frac{A_z(p \rightarrow q)}{A_z(p' \rightarrow q')} \frac{A_z(p' \rightarrow)}{A_z(p \rightarrow)} \frac{X_z(g \rightarrow p)(T_e)}{X_z(g \rightarrow p')(T_e)} \left[1 + n_e \frac{X_z(p' \rightarrow)}{A_z(p' \rightarrow)} \right] \Rightarrow n_e$$

HFR+CPOL preliminary results

HFR method

General procedure [Cowan, R. D. ,1981]

- Solve $H\Psi = E\Psi$ where $H = \sum_{i=1}^N \left(-\frac{1}{2}\Delta_i + V(r_i) \right)$ (central field approximation)
- $H_i\varphi_i = E_i\varphi_i \rightarrow \varphi_i(r_i, \theta_i, \phi_i, s_i) = \frac{1}{r_i} P_{n_il_i}(r_i) Y_{l_i}^{m_i}(\theta_i, \phi_i) \sigma_{m_{s_i}}(s_i)$
- $P_{n_il_i}(r_i)$? \rightarrow solve Hartree-Fock equations (Self-Consistent Field method)
- HF equations obtained by variationnal principle on the average energy of each eletronic configuration
- Atomic State Functions (ASFs) : $\Psi(\alpha, P, J, M_J) = \sum_{r=1}^{n_c} c_r \Phi(\alpha_r, P, L_r, S_r, J, M_J)$

Configuration State Functions (CSFs) are built thanks to Slater determinants

HFR+CPOL method

Core polarisation correction

- Valence electron correlations represented by configuration interactions (CI) and other correlations by core-polarisation potential
- Quinet, P. et al [1999, 2002]: pseudo potentiel have one-body and two-body part :

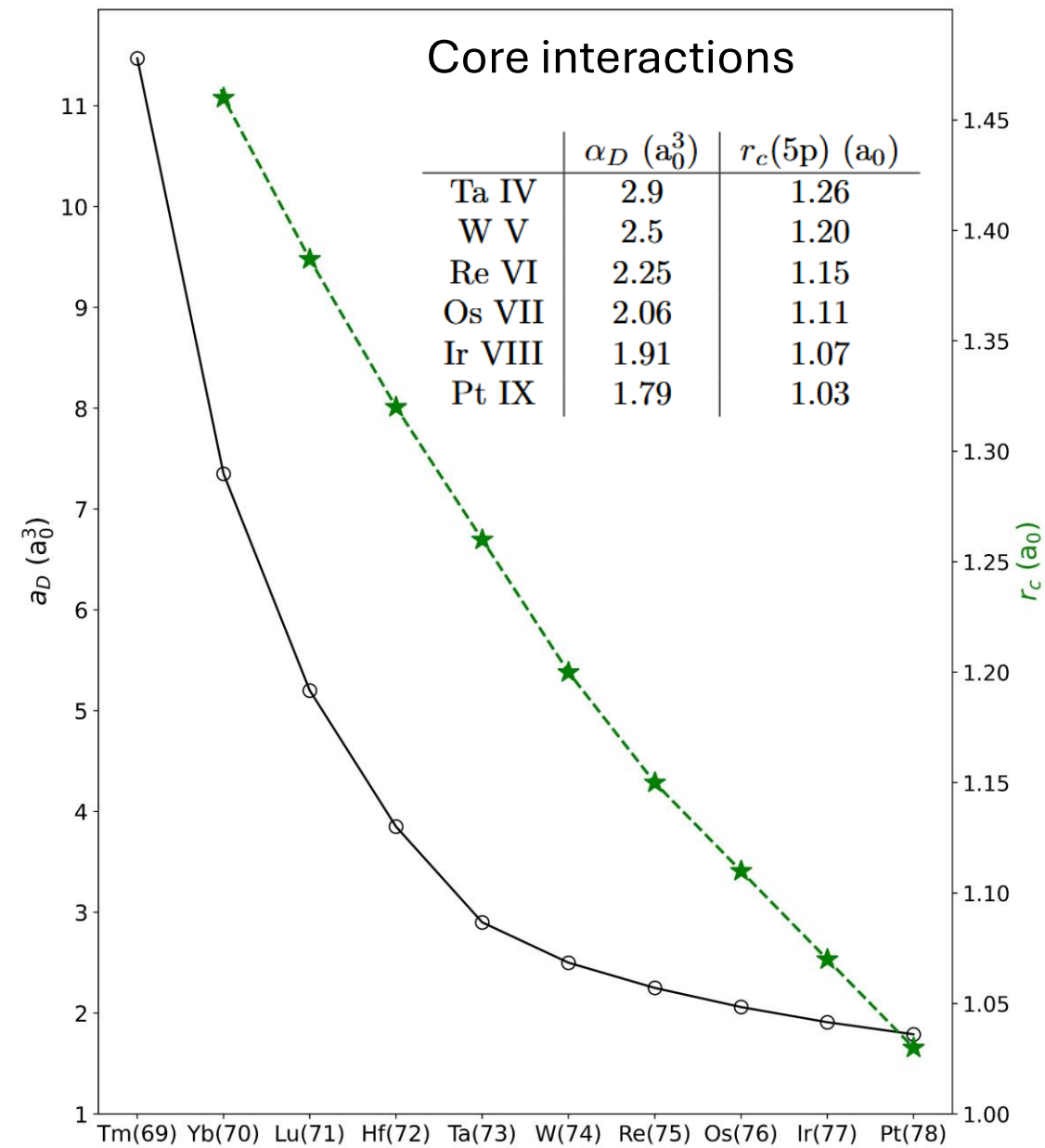
$$\triangleright V_{P1} = -\frac{1}{2} \alpha_D \sum_{i=1}^N \frac{r_i^2}{(r_i^2 + r_c^2)^3} \text{ and } V_{P2} = -\alpha_D \sum_{i>j} \frac{\vec{r}_i \cdot \vec{r}_j}{[(r_i^2 + r_c^2)(r_j^2 + r_c^2)]^{3/2}}$$

$\triangleright \alpha_D$: dipole polarisability; r_c : ionic core radius

HFR+CPOL Model

Valence-Valence interactions

Even parity	Odd parity
5d ²	6p6f
5d6s	6p7f
5d7s	6d ²
6s ²	6d7s
5d6d	6d7d
5d7d	7s ²
6s7s	7p ²
6s6d	7s7d
6s7d	7p5f
6p7p	7p6f
6p ²	7p7f
6p5f	
	5d6p 6p6d
	6s6p 6p7d
	5d7p 6d7p
	5d5f 6d5f
	5d6f 6d6f
	5d7f 6d7f
	6s7p 7s5f
	6s5f 7s6f
	6s6f 7s7f
	6s7f 7s7p
	6p7s 7s7d



Least squares method

- Minimise difference between computed energy levels and observed ones with spin-orbit and Slater parameters
- Accuracy of the fit: $\sigma = \left[\frac{\sum_k (E^k - T^k)^2}{N_k - N_p} \right]^{1/2}$, where E^k : energy eigenvalues; T^k : observed energies; N_k : number of fitted levels; N_p : number of fitted parameters

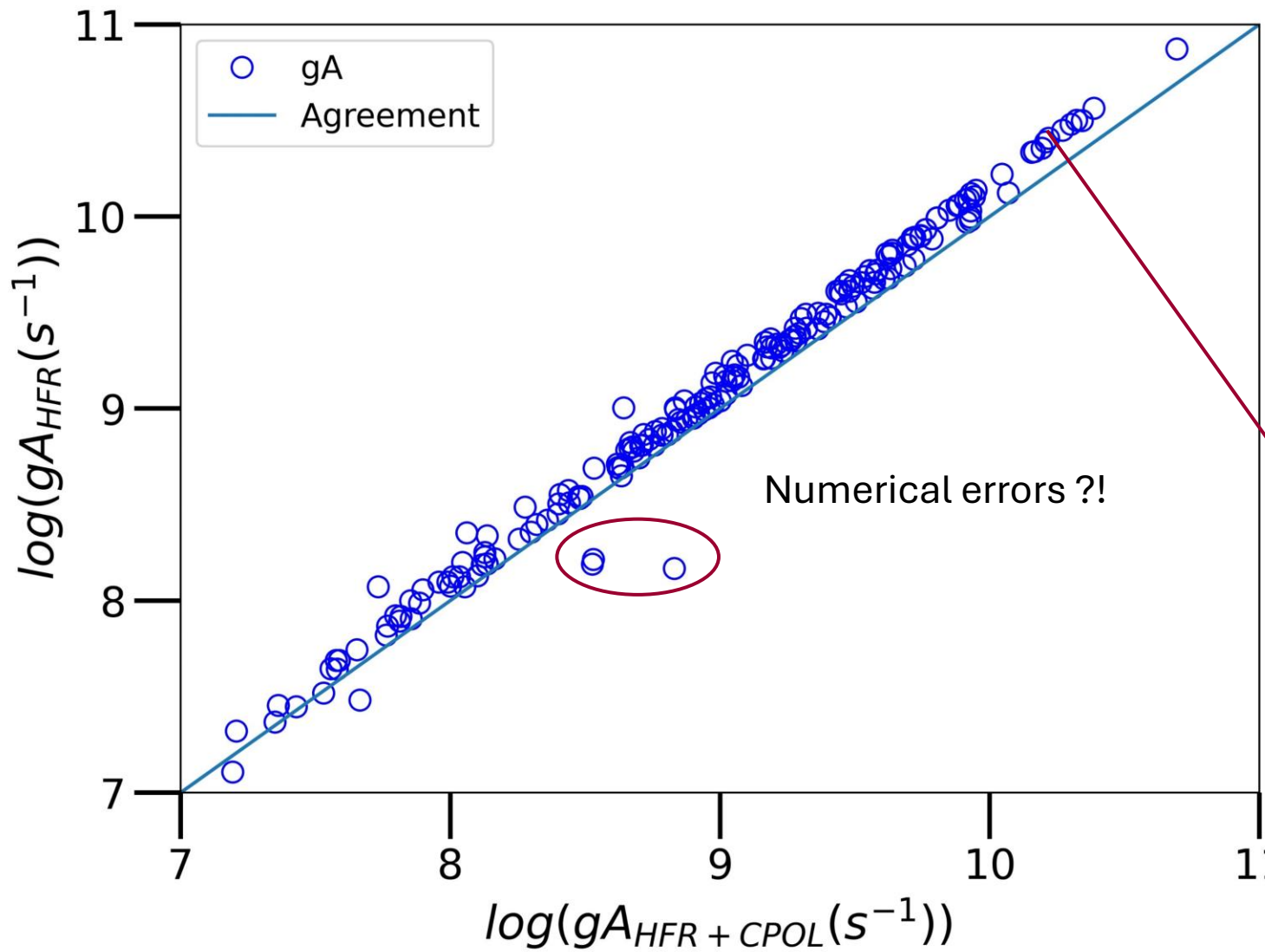
	Even parity		Odd parity	
	nbr of fitted levels	σ (cm $^{-1}$)	nbr of fitted levels	σ (cm $^{-1}$)
Ta IV	14	23	44	145
W V	13	20	44	132
Re VI	13	30	29	347

[Churilov, S.S. et all, 1996 ; Meijer, F.G and Metsch, 1978 ; Kildiyarova, R.R et all, 1996 ; Kramida , A. et all, 2024 ; Sugar, J. et all, 1994 ; Yoca, S.E et all, 2012]

Radiative decay rates

Ta IV

[Churilov, S.S. et all, 1996 ; Meijer, F.G and Metsch, 1978 ; Kildiyarova, R.R et all, 1996]



213 observed electric dipole lines
between 551.422 – 3076.060 Å

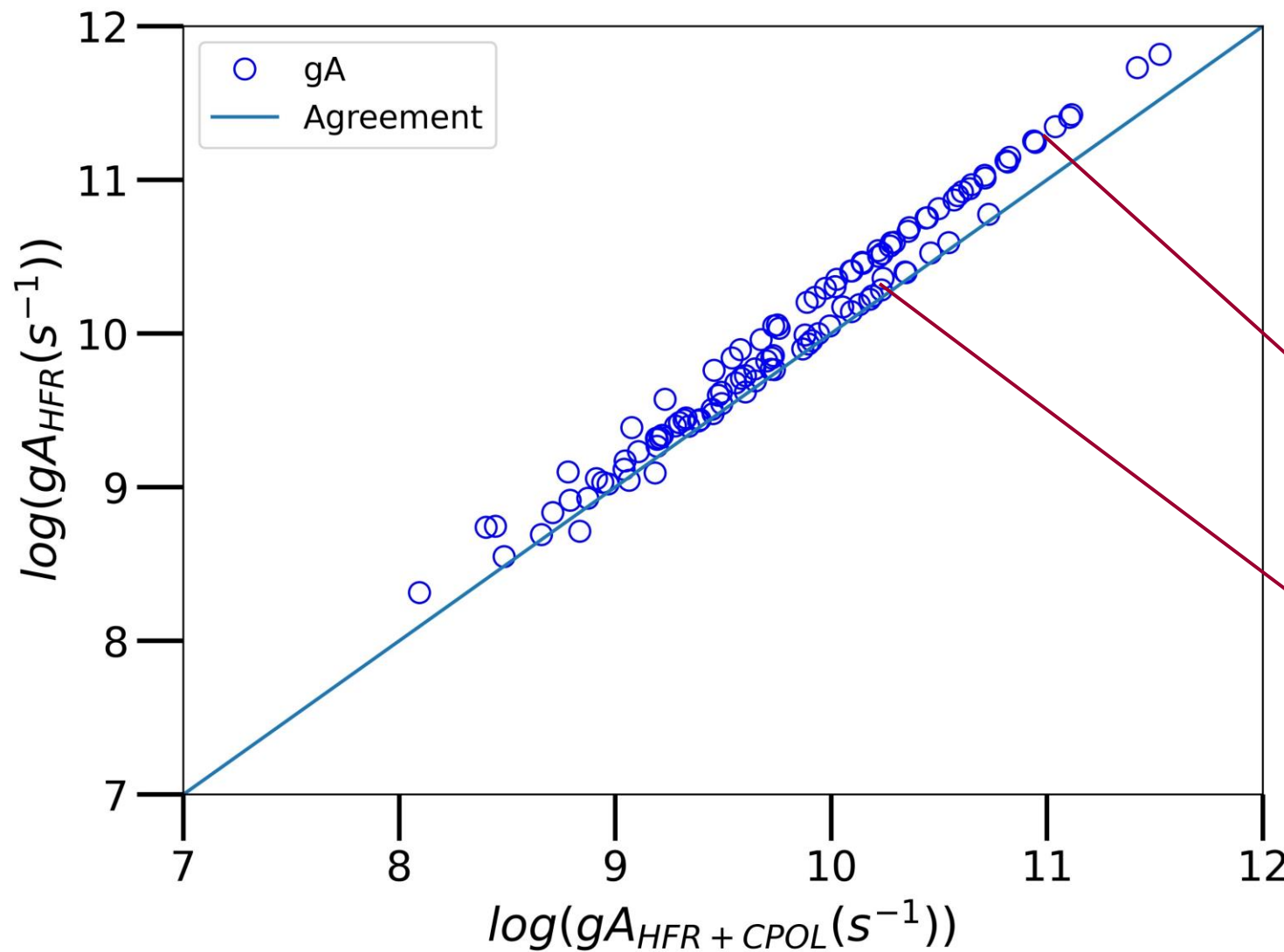
Mean ratio $gA_{HFR+CPOL}/gA_{HFR}=0.83$

CPOL corrections reduce gA -values of
about 20%, as expected.

For $5d \rightarrow 5f, 7p$ ($5d^2 \rightarrow 5d5f, 5d7p$) :
reduction is on average 30%

Re VI

112 observed electric dipole lines between 332.044 – 1513.957 Å [Sugar, J. et all, 1994]

Mean ratio $gA_{HFR+CPOL}/gA_{HFR}=0.69$

CPOL corrections reduce more gA-values of about 30%

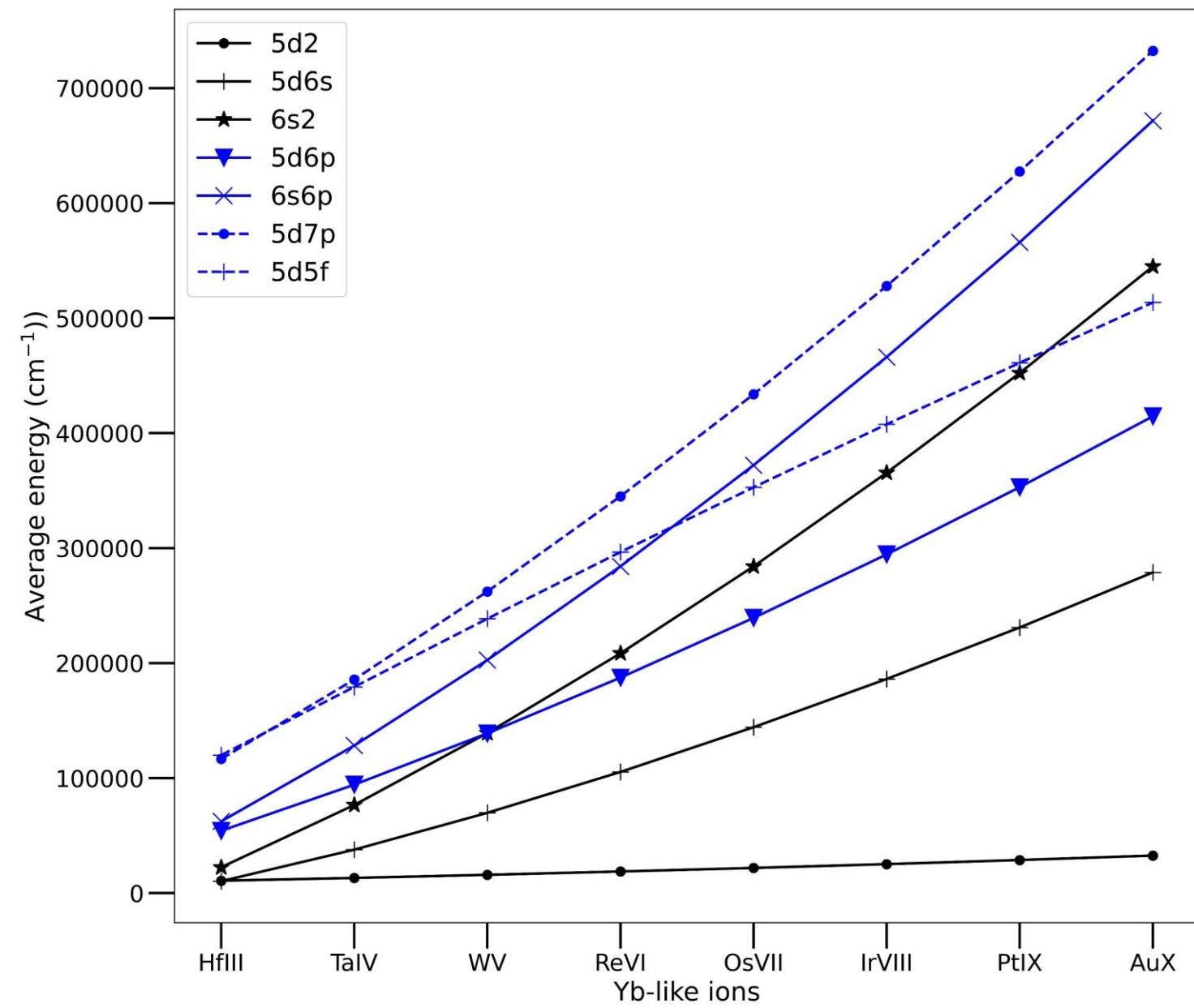
For $5d \rightarrow 5f$ ($5d^2 \rightarrow 5d5f$) :
mean ratio $gA_{HFR+CPOL}/gA_{HFR} = 0.50$

For $5d, 6s \rightarrow 6p$ ($5d^2, 5d6s \rightarrow 5d6p$) :
mean ratio $gA_{HFR+CPOL}/gA_{HFR} = 0.85$

$\Rightarrow E_{av}$ of configurations with open 4f,5p core orbital closer to valence configurations

Configuration Interactions

The atomic level structure more spread out with increasing ionic charge state → on average less mixing in the level composition

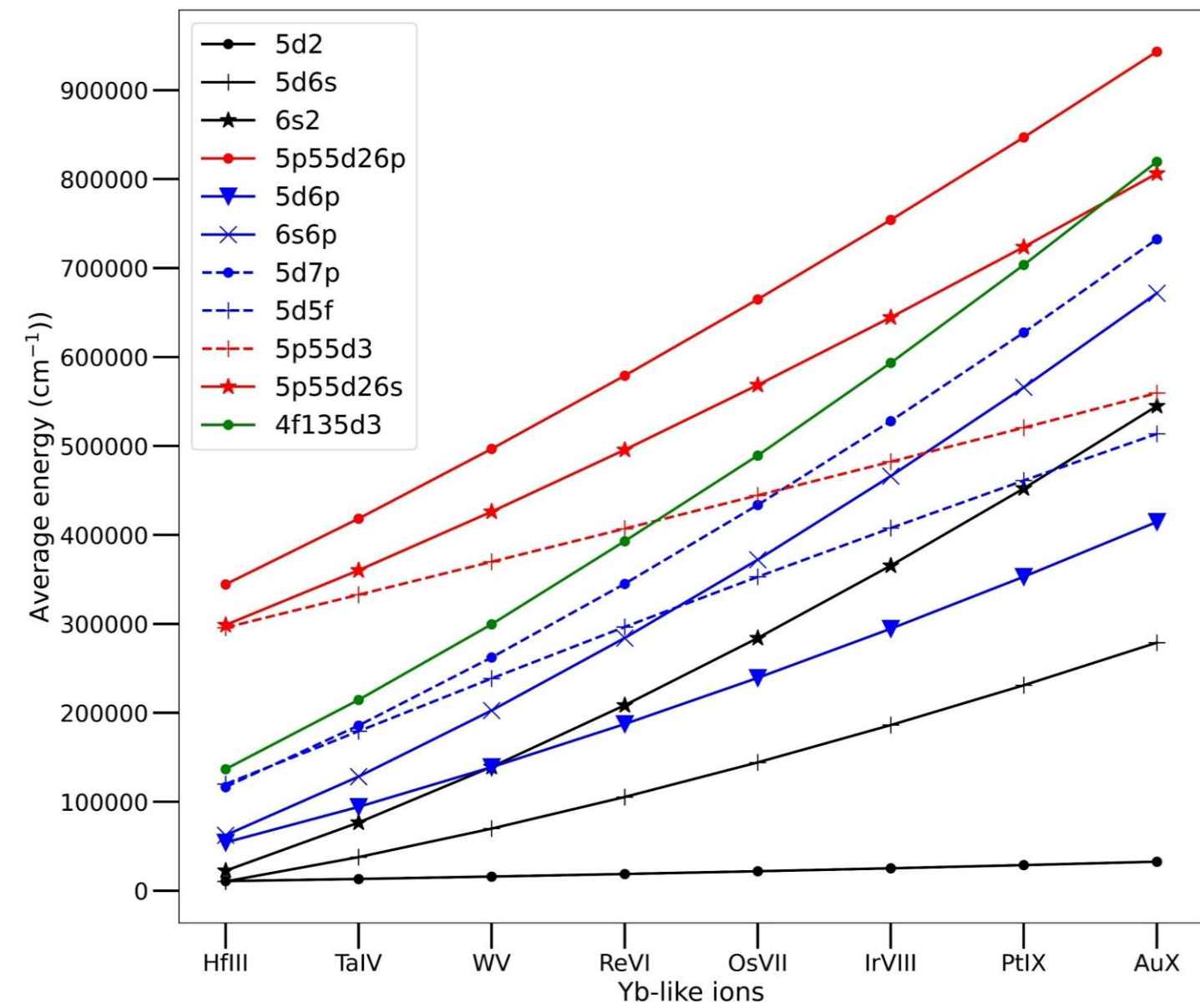


Core-valence correlations

$5p^5 5d^3$ closer to (and overlap) $5d7p$,
 $6s6p$ and $5d5f$

→ core-valence correlations with a
 pseudo potential no longer valid

→ need to introduce explicitly the
 configurations with an open $5p, 4f$ core
 orbitals in our model (through CI)



MCDHF preliminary results

MCDHF method

General procedure [Grant, I. P., 2007]

- $H_{DC} = \sum_{i=1}^N h_{D_i}$ with $h_{D_i} = c\vec{\alpha} \cdot \vec{p}_i + (\beta - 1)c^2 + V(r_i)$ ($\alpha^j = \gamma^0\gamma^j$ and $\beta = \gamma^0$)
- Each electron: $h_D\varphi = E\varphi \rightarrow \varphi(r, \theta, \phi) = \frac{1}{r} \begin{pmatrix} P_{n,\kappa}(r)\chi_{\kappa,m}(\theta, \phi) \\ iQ_{n,\kappa}(r)\chi_{\kappa,m}(\theta, \phi) \end{pmatrix}$ where $P_{n,\kappa}(r)$ and $Q_{n,\kappa}(r)$ are **large** and **small radial part**, respectively.
- $P_{n,\kappa}(r), Q_{n,\kappa}(r) ? \rightarrow$ solve MCDHF equations (Self-Consistent Field method)
- CI: (ASF) $\Psi(P, J, M) = \sum_{r=1}^{n_c} c_r \Phi(\gamma_r, P, J, M)$

MCDHF Models

- The Atomic State Functions (ASFs) are built with the Active Set approach $(n_{max}l, n'_{max}l', \dots)$:
- Optimisation of all orbitals (5s,5p,5d,4f) on the $5d^2\ ^3F_2$ ground state
- MR : (re)optimize valence orbitals on all levels
- VV1,2,3 : ONLY « new » correlation orbitals are optimized on all levels of the MR
- CV,CC : Relativistic Configuration Interactions (RCI) calculations

	Even parity	Number of CSFs
MR ($5d^2, 5d6s, 6s^2$)	($6s, 5p, 5d, 4f$)	14
VV1	SD(MR) \rightarrow ($7s, 6p, 6d, 5f$)	81
VV2	SD(MR) \rightarrow ($8s, 7p, 7d, 6f$)	225
VV3	SD(MR) \rightarrow ($9s, 8p, 8d, 7f$)	446
CV1 (RCI)	SrD (MR{4f}) \rightarrow ($9s, 8p, 8d, 7f$)	29 249
CV2 (RCI)	SrD (MR{4f,5p}) \rightarrow ($9s, 8p, 8d, 7f$)	47 273
CV3 (RCI)	SrD (MR{4f,5p,5s}) \rightarrow ($9s, 8p, 8d, 7f$)	53 778
CC1 (RCI)	SD (MR{4f(2)}) \rightarrow ($9s, 8p, 8d, 7f$)	274 515
CC2 (RCI)	SD (MR{4f,5p}) \rightarrow ($9s, 8p, 8d, 7f$)	367 215
CC3 (RCI)	SD (MR{4f,5p}) + SrD (MR{5s}) \rightarrow ($9s, 8p, 8d, 7f$)	373 720
	Odd parity	Number of CSFs
MR ($5d6p, 6s6p, 5d5f, 5d7p$)	($6s, 7p, 5d, 5f$)	47
VV1	SD(SR) \rightarrow ($7s, 8p, 6d, 6f$)	188
VV2	SD(SR) \rightarrow ($8s, 9p, 7d, 7f$)	399
VV3	SD(SR) \rightarrow ($9s, 10p, 8d, 8f$)	688
CV1 (RCI)	SrD (MR{4f}) \rightarrow ($9s, 10p, 8d, 8f$)	115 980
CV2 (RCI)	SrD (MR{4f,5p}) \rightarrow ($9s, 10p, 8d, 8f$)	184 664
CV3 (RCI)	SrD (MR{4f,5p,5s}) \rightarrow ($9s, 10p, 8d, 8f$)	208 892
CC1 (RCI)	SD (MR{4f(2)}) \rightarrow ($9s, 10p, 8d, 8f$)	1 980 405
CC2 (RCI)	SD (MR{4f,5p}) \rightarrow ($9s, 10p, 8d, 8f$)	2 574 277
CC3 (RCI)	SD (MR{4f,5p}) + SrD (MR{5s}) \rightarrow ($9s, 10p, 8d, 8f$)	2 602 097

Convergence of the models

Ta IV

	Even parity		Odd parity	
	$\Delta E/E_{obs}$	$\Delta E/E_{prev}$	$\Delta E/E_{obs}$	$\Delta E/E_{prev}$
MR	9.99%		1.53%	
VV1	4.12%	5.91%	1.52%	0.35%
VV2	3.75%	0.39%	1.56%	0.05%
VV3	3.69%	0.06%	1.57%	0.01%
CV1	5.25%	1.86%	0.71%	1.44%
CV2	7.71%	3.35%	2.11%	2.08%
CV3	6.40%	1.31%	2.33%	0.21%
CC1	6.59%	1.60%	10.60%	9.48%
CC2	6.90%	0.86%	5.10%	2.83%
CC3	5.65%	0.88%	5.23%	2.74%

303 transitions over 317 have a ratio $gA_{HFR+CPOL}/gA_{MCDHF} < 10$ with a mean ratio 1.39

299 transitions over 317 have a ratio $gA_{HFR+CPOL}/gA_{MCDHF} < 10$ with a mean ratio 1.26

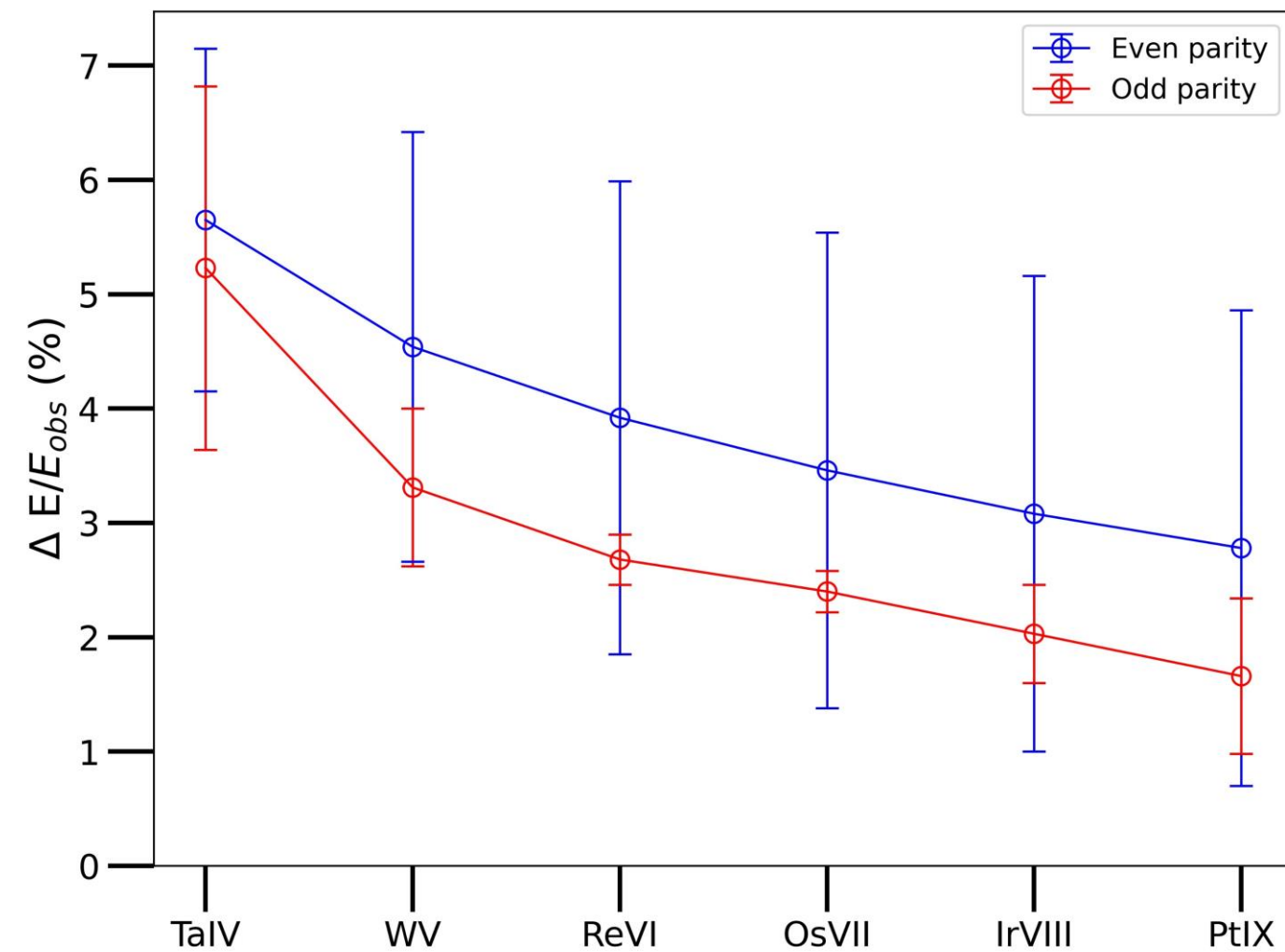
	Even parity		Number of CSFs
MR (5d ² ,5d6s,6s ²)	(6s,5p,5d,4f)		14
VV1	SD(MR) → (7s,6p,6d,5f)		81
VV2	SD(MR) → (8s,7p,7d,6f)		225
VV3	SD(MR) → (9s,8p,8d,7f)		446
CV1 (RCI)	SrD (MR{4f}) → (9s,8p,8d,7f)		29 249
CV2 (RCI)	SrD (MR{4f,5p}) → (9s,8p,8d,7f)		47 273
CV3 (RCI)	SrD (MR{4f,5p,5s}) → (9s,8p,8d,7f)		53 778
CC1 (RCI)	SD (MR{4f(2)}) → (9s,8p,8d,7f)		274 515
CC2 (RCI)	SD (MR{4f,5p}) → (9s,8p,8d,7f)		367 215
CC3 (RCI)	SD (MR{4f,5p}) + SrD (MR{5s}) → (9s,8p,8d,7f)		373 720
	Odd parity		Number of CSFs
	MR (5d6p,6s6p,5d5f,5d7p)		
VV1	(6s,7p,5d,5f)		47
VV2	SD(SR) → (7s,8p,6d,6f)		188
VV3	SD(SR) → (8s,9p,7d,7f)		399
CV1 (RCI)	SD(SR) → (9s,10p,8d,8f)		688
CV2 (RCI)	SrD (MR{4f}) → (9s,10p,8d,8f)		115 980
CV3 (RCI)	SrD (MR{4f,5p}) → (9s,10p,8d,8f)		184 664
CC1 (RCI)	SrD (MR{4f,5p,5s}) → (9s,10p,8d,8f)		208 892
CC2 (RCI)	SD (MR{4f(2)}) → (9s,10p,8d,8f)		1 980 405
CC3 (RCI)	SD (MR{4f,5p}) → (9s,10p,8d,8f)		2 574 277
	SD (MR{4f,5p}) + SrD (MR{5s}) → (9s,10p,8d,8f)		2 602 097

Even parity (CC3) : SD (MR {4f,5p}) + SrD (MR {5s}) → (9s,8p,8d,7f)

Odd parity (CC3) : SD (MR {4f,5p}) + SrD (MR {5s}) → (9s,10p,8d,8f)

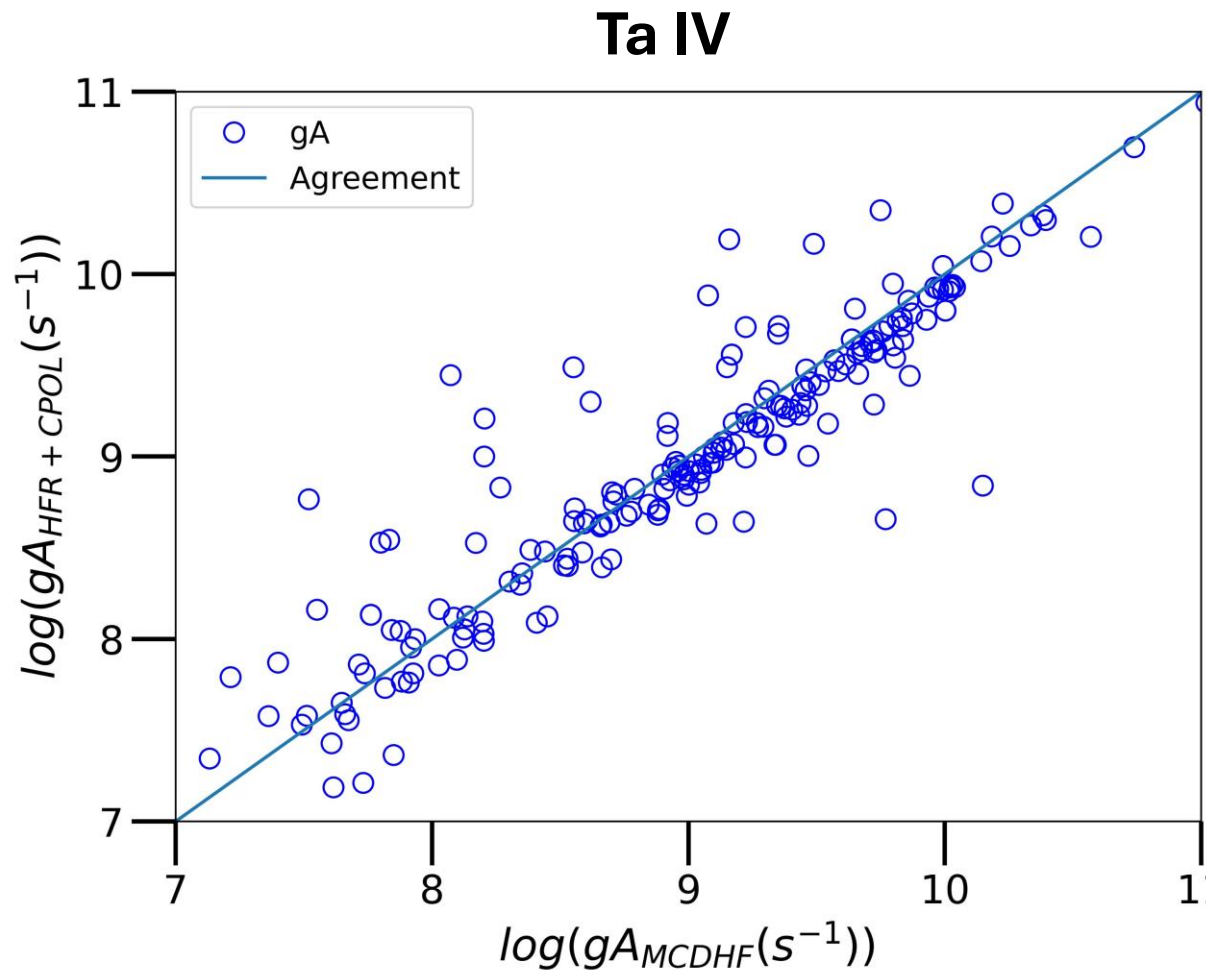
	$\Delta E/E_{obs}$	
	Even parity	Odd parity
TaIV	5.65%	5.23%
WV	4.54%	3.31%
ReVI	3.92%	2.68%
OsVII	3.46%	2.40%
IrVIII	3.08%	2.03%
PtIX	2.78%	1.80%

$5d^2 \ ^3P_0, 5d^2 \ ^1S_0 : \Delta E/E_{obs} > 8\%$



Comparisons between HFR+CPOL and MCDHF gA's

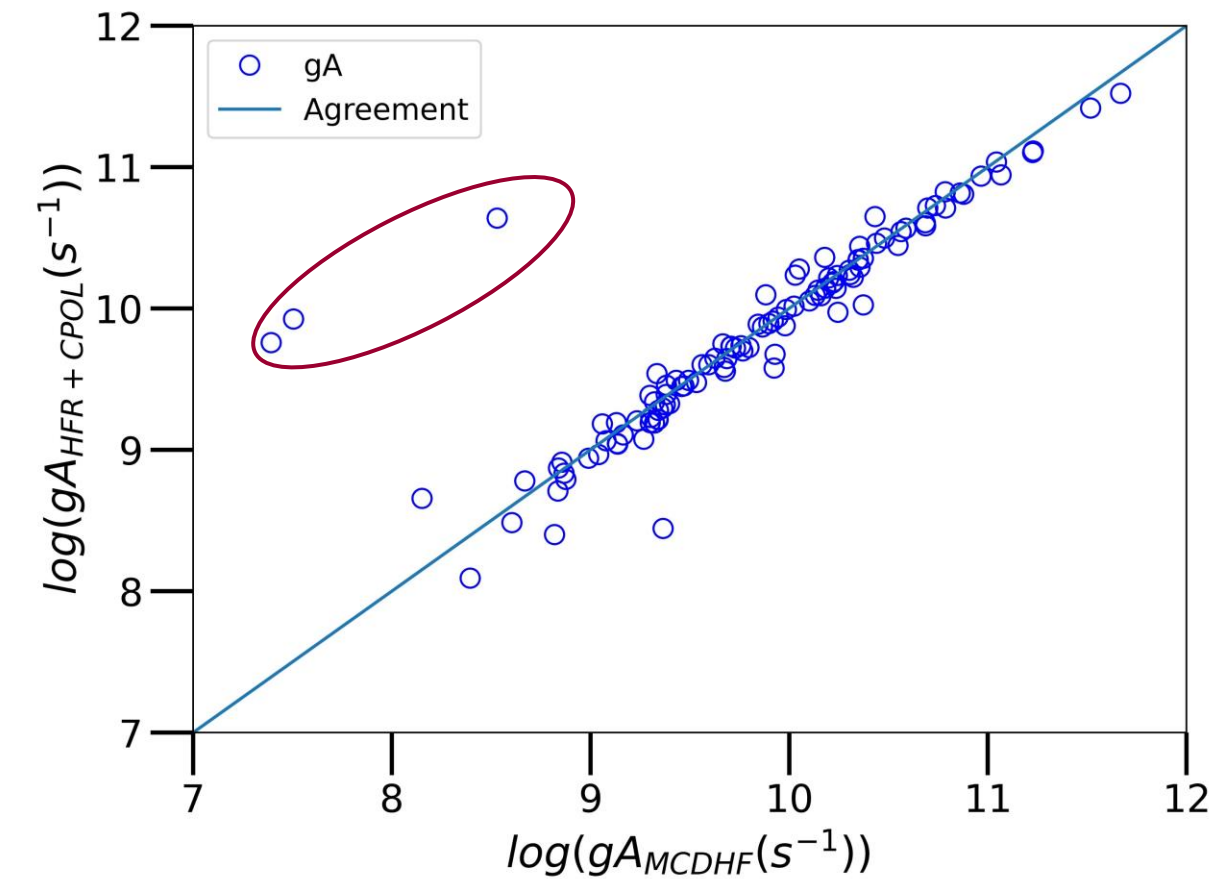
Ta IV



Mean relative difference $\Delta gA / \max(gA_{HFR+CPOL}; gA_{MCDHF}) = 32.3\%$

Mean ratio $gA_{HFR+CPOL} / gA_{MCDHF} = 2.16 \pm 2.30$

Re VI



$\Delta gA / \max(gA_{HFR+CPOL}; gA_{MCDHF}) = 18.9\%$

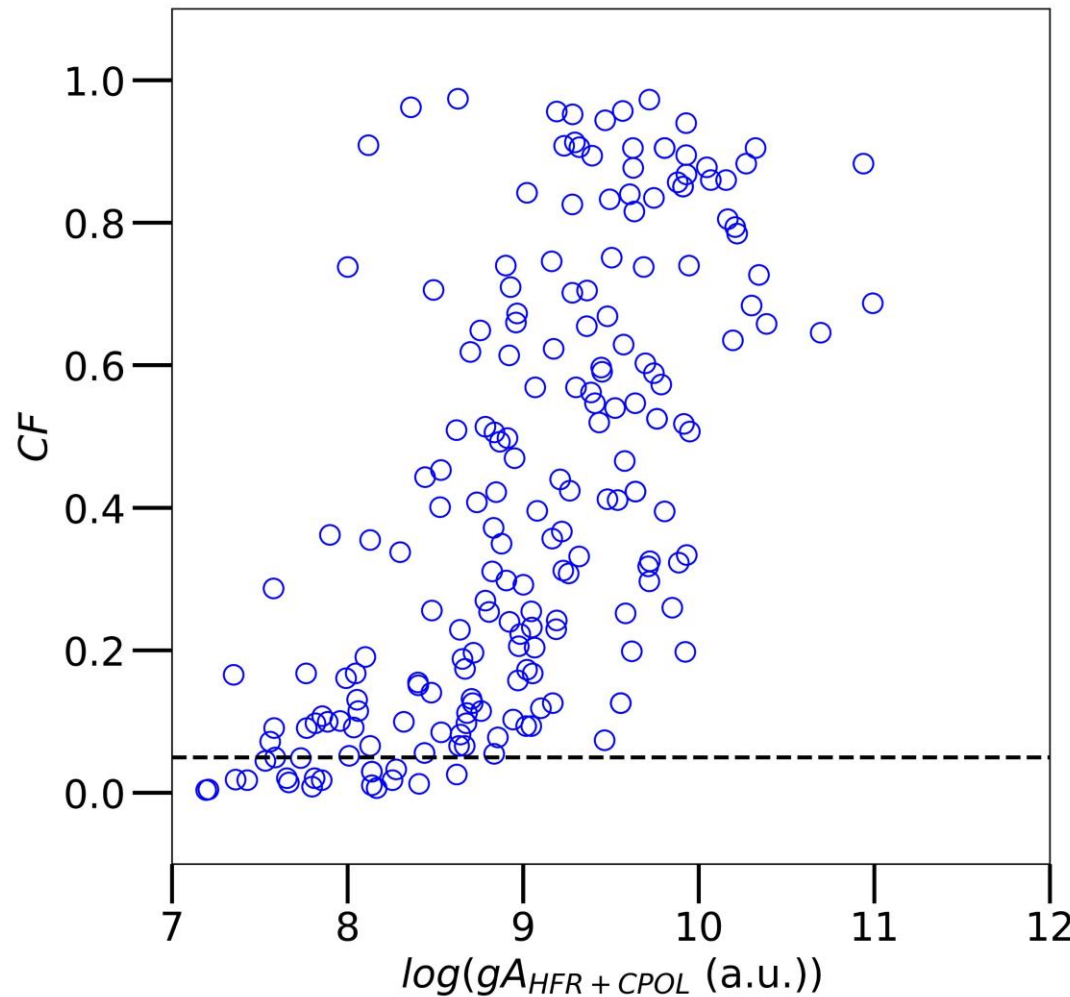
$gA_{HFR+CPOL} / gA_{MCDHF} = 6.52 \pm 10.81$
(three high ratios : 129, 232 and 263)

All gA (and gf) computed in both methods are not reliable

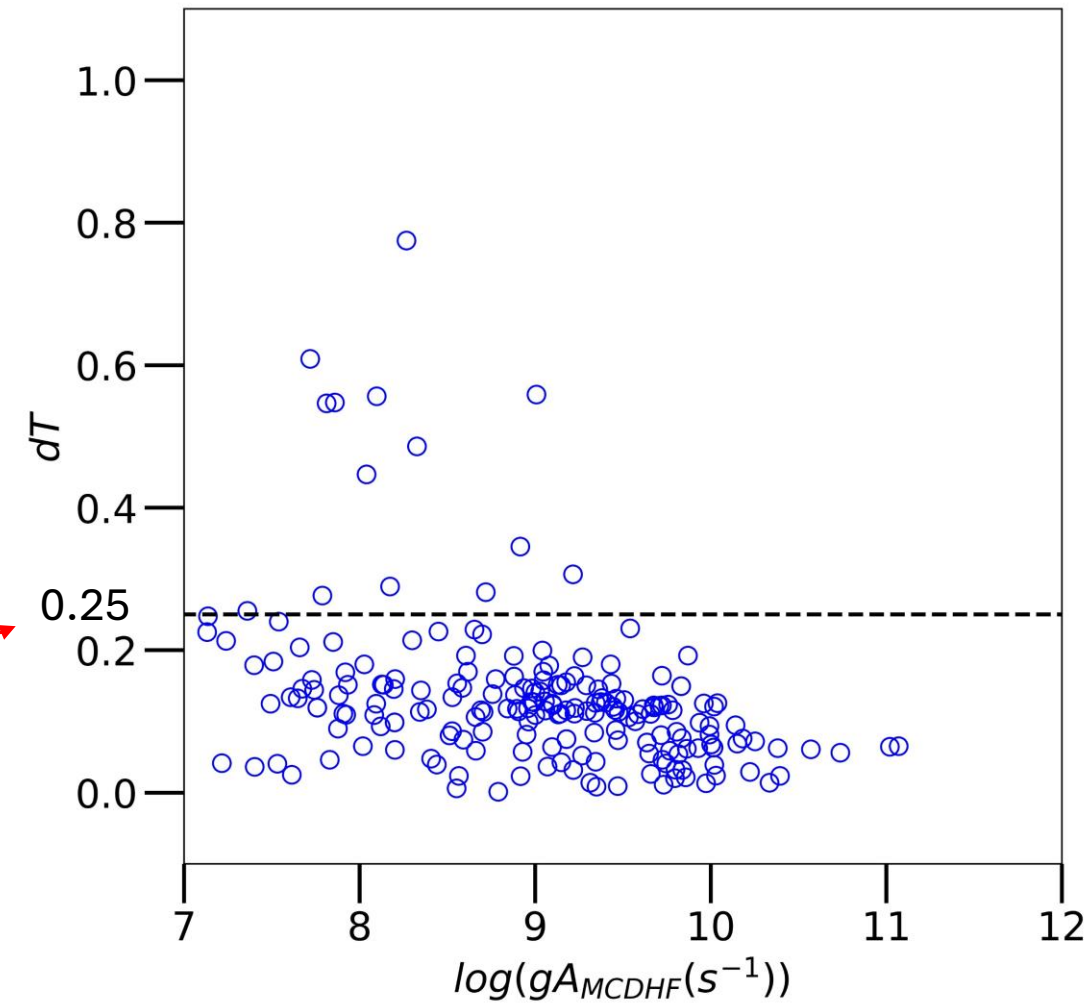
Ta IV

Cancellation Factor $CF_{ij} = \left(\frac{\sum_b \sum_c y_j^b y_i^c \langle \psi_c | \mathbf{P}^{(1)} | \psi_b \rangle}{\sum_b \sum_c |y_j^b y_i^c \langle \psi_c | \mathbf{P}^{(1)} | \psi_b \rangle|} \right)^2$ **Uncertainty of MCDHF transition rates :** $dT = \frac{|A_B - A_C|}{\max(A_B, A_C)}$

[Cowan, R. D., 1981]



0.05
[Cowan, R. D., 1981]

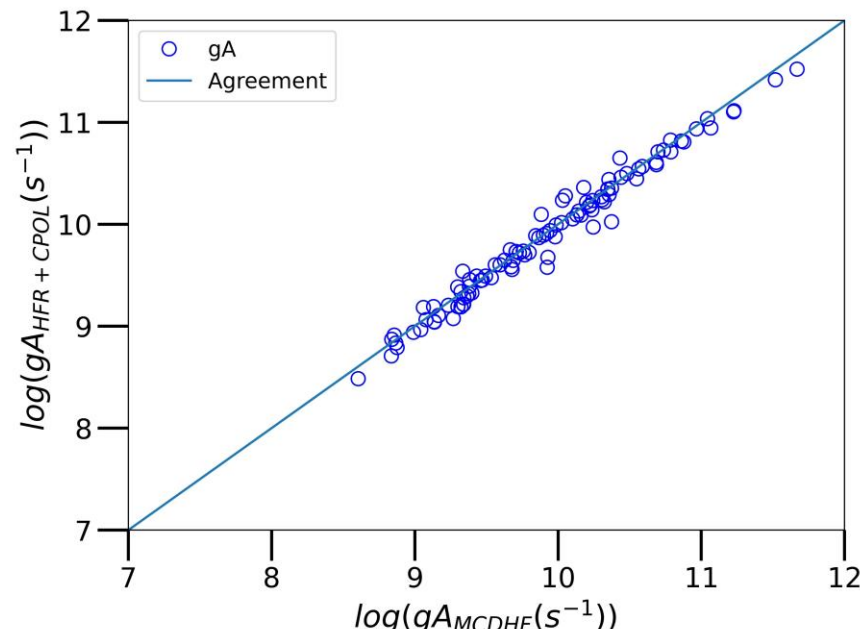
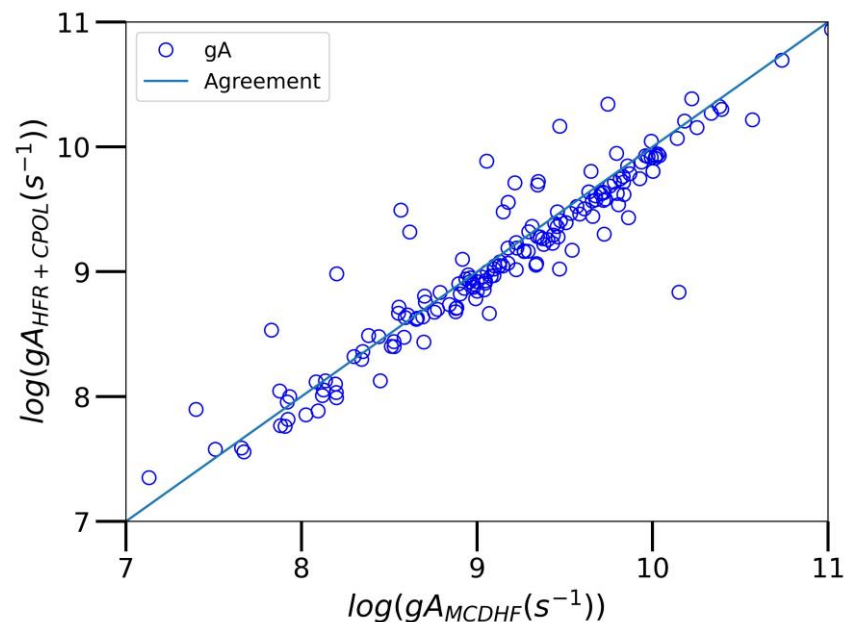


Ta IV

- It remains 170 transitions (among 213) with $CF > 0.05$ and $dT < 0.25$
- The uncertainty on the HFR+CPOL and MCDHF results estimated on average 26%
 - ↳ $\frac{\Delta gA}{\max}$ where $\Delta gA = |gA_{HFR+CPOL} - gA_{MCDHF}|$
and $\max=\max(gA_{HFR+CPOL}; gA_{MCDHF})$
- Mean ratio $gA_{HFR+CPOL}/gA_{MCDHF} = 1.12 \pm 0.54$

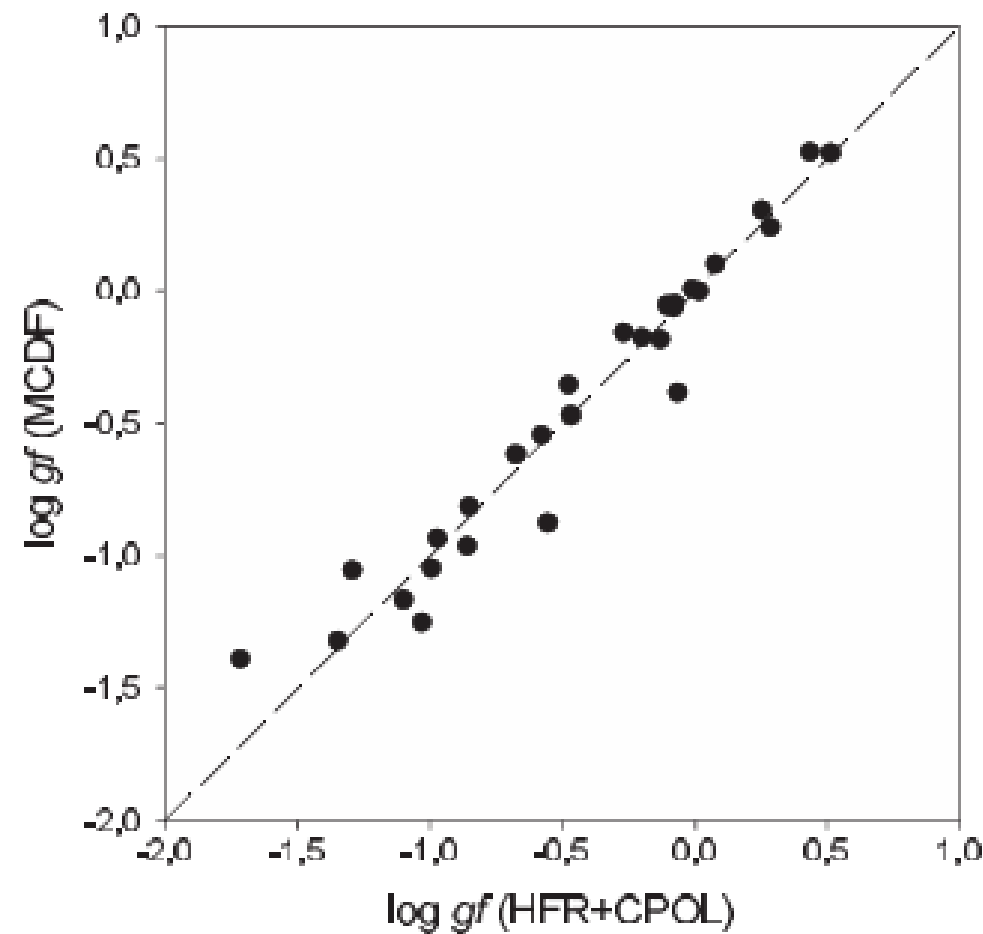
Re VI

- It remains 101 transitions (among 112) with $CF > 0.05$ and $dT < 0.25$
- The uncertainty estimated on average 15% with a mean ratio 0.96 ± 0.16



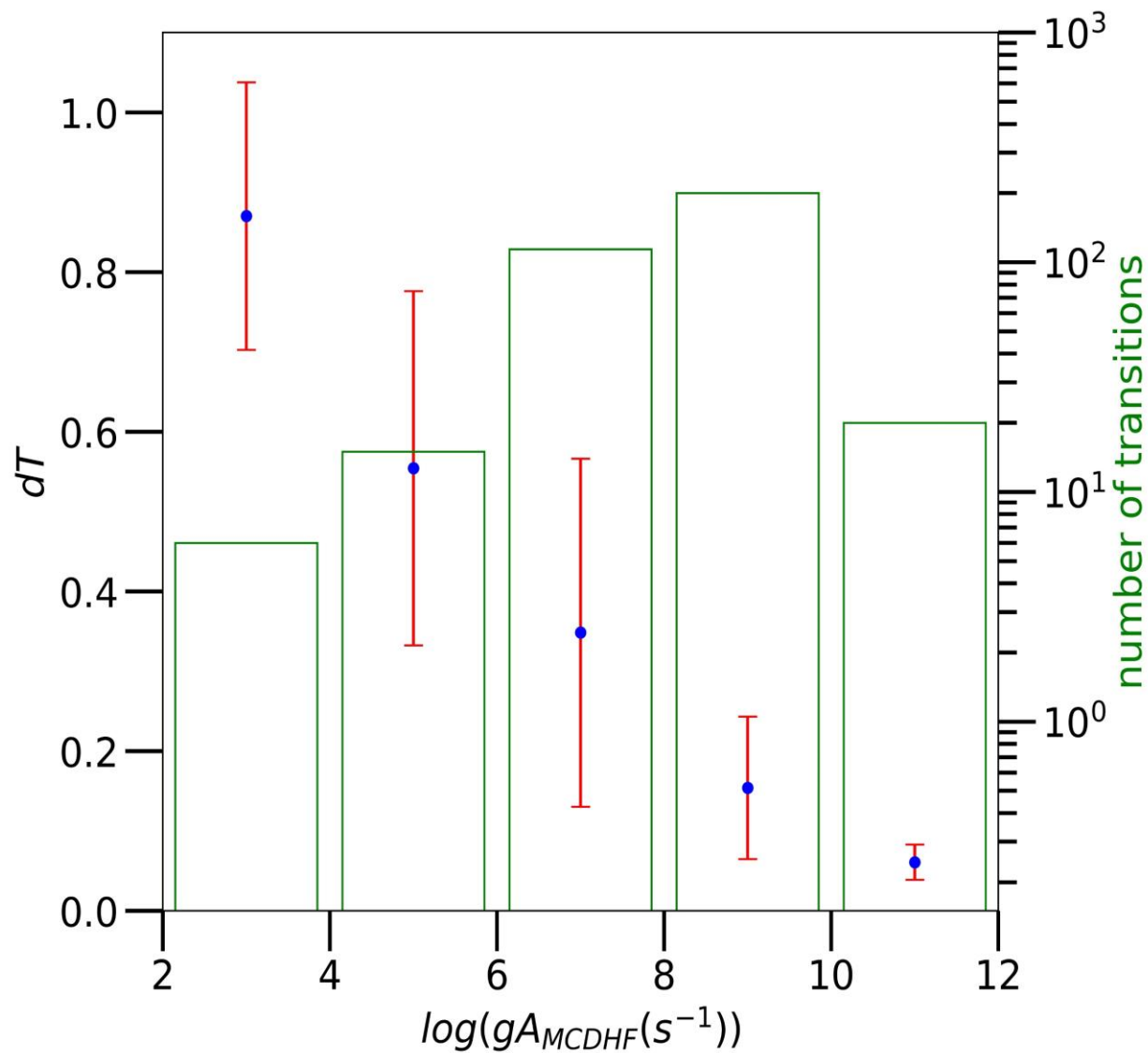
W V

- 193 dipole electric lines between 390 – 2190 Å [Kramida, A. et all, 2024]
- For 5d²-5d6p and 5d6s-5d6p transitions :
- $\Delta gf = |gf_{HFR+CPOL} - gf_{MCDHF}| = 21\% (<30\%)$ [Yoca, S.E et all, 2012]



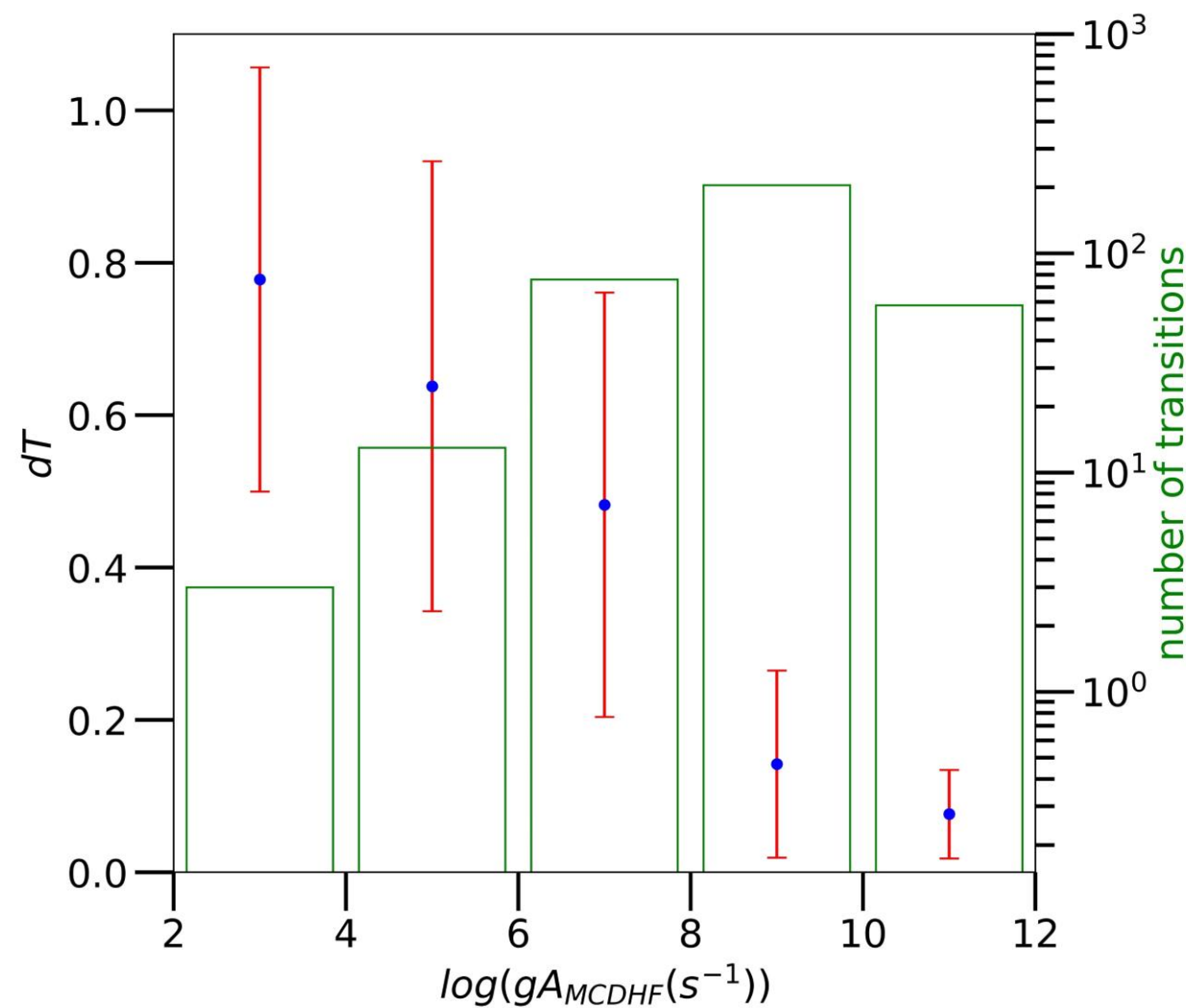
Ta IV

- All 355 transitions computed in the MCDHF method
- ⇒ 251 transitions have $dT < 0.25$
- ⇒ The more intense the transitions, the lower the dT value



Re VI

- All 355 transitions computed in the MCDHF method
 - ⇒ 253 transitions have $dT < 0.25$
 - ⇒ The more intense the transitions, the lower the dT value



- Origin of Tantalum up to Platinium in the fusion plasma (tungsten transmutation)
- Compute radiative parameters with HFR+CPOL method + least squares ajustement
- Increasing the ionic charge, configurations with an open 4f,5p orbitals begin to overlap the valence configurations → Introduce explicitly these configurations ?!
- Good agreement between HFR+CPOL and MCDHF method and comparisons (170 transitions for TaIV and 101 for ReVI) allow to estimate uncertainty (TaIV:26%; ReVI:15%)
 - set of new atomic data for TaIV → PtIX for plasma diagnostics
- Same procedure for higher ionic charge state of tungsten transmutation products (Ta, Re, Os, Ir, Pt)
- However, few atomic data published



THANK YOU !



Bibliography

- Biémont, E., Garnir, H. P., Palmeri, P., Quinet, P., Li, Z. S., Zhang, Z. G., & Svanberg, S. (2001). Core-polarization effects and radiative lifetime measurements in PrIII. *Physical Review A*, 64, 022503.
- Churilov, S. S., Kildiyarova, R. R., and Joshi, Y. N. Analyses of the 5d₂–5d7p transitions in the Ta IV and W V spectra. *Canadian Journal of Physics* 74, 3-4 (1996), 145–149.
- Cowan, R.D. *The Theory of Atomic Structure and Spectra*; University of California Press: Berkeley, CA, USA, 1981.
- Fraga, S., Karwowski, J., & Saxena, K. M. S. (1976). *Handbook of atomic data*. Elsevier, Amsterdam.
- Gilbert, N.R.; Sublet, J.C. Neutron-induced transmutation effects in W and W-alloys in a fusion environment. *Nucl. Fusion* 2011, 51, 043005.
- Grant, I.P. *Relativistic Quantum Theory of Atoms and Molecules*; Springer: New York, NY, USA, 2007.
- Kildiyarova, R. R., Churilov, S. S., Joshi, Y. N., & Ryabtsev, A. N. (1996). Analysis of the 5d5f configuration of trebly ionized tantalum and quadruply ionized tungsten: Ta IV and W V. *Physica Scripta*, 53 (4), 454.
- Kramida A., Ralchenko Yu., Reader J., and NIST ASD Team. Atomic Spectra Database. National Institute of Standards and Technology, Gaithersburg, 2024. URL. <https://www.nist.gov/pml/atomic-spectra-database>
- Kunze, H.-J. (2009). *Introduction to Plasma Spectroscopy* (Vol. 56). Springer
- Meijer, F. G., and Metsch, B. C. The analysis of the fourth spectrum of tantalum, Ta IV. *Physica B+C* 94, 2 (1978), 259–269

Bibliography

- Quinet, P., Palmeri, P., Biémont, E., Li, Z. S., Zhang, Z. G., & Svanberg, S. (2002). Radiative lifetime measurements and transition probability calculations in lanthanide ions. *Journal of Alloys and Compounds*, 344 (1), 255–259
- Quinet, P., Palmeri, P., Biémont, E., McCurdy, M. M., Rieger, G., Pinnington, E. H., Wickliffe, M. E., & Lawler, J. E. (1999). Experimental and theoretical radiative lifetimes, branching fractions and oscillator strengths in Lu ii. *Monthly Notices of the Royal Astronomical Society*, 307 (4), 934–940.
- Raassen, A. J. J., Azarov, V. I., Uylings, P. H. M., Joshi, Y. N., Tchang-Brillet, L., and Ryabtsev, A. N. Analysis of the spectrum of five times ionized osmium (Os VI). *Physica Scripta* 54, 1 (1996), 56.
- Sugar, J., Wyart, J.-F., Hof, G. J. v. h., & Joshi, Y. N. (1994). Spectrum and energy levels of five-times-ionized rhenium. *JOSA B*, 11 (12), 2327–2332.
- Yoca, S. E., Quinet, P., Palmeri, P., and Biémont, Comparative semi-empirical and ab initio atomic structure calculations in Yb-like tungsten W⁴⁺. *Journal of Physics B: Atomic, Molecular and Optical Physics* 45, 6 (2012), 065001